HHS Public Access

Author manuscript

Int J Biochem Cell Biol. Author manuscript; available in PMC 2019 January 01.

Published in final edited form as:

Int J Biochem Cell Biol. 2018 January ; 94: 119–124. doi:10.1016/j.biocel.2017.12.001.

Long-Term Pulmonary and Cardiovascular Morbidities of Neonatal Hyperoxia Exposure in Mice

Renuka T. Menon[1], **Amrit Kumar Shrestha**[1], **Corey L. Reynolds**[2], **Roberto Barrios**[3], and **Binoy Shivanna**[1,*]

[1]Section of Neonatology, Department of Pediatrics, Baylor College of Medicine, Houston, Texas, USA

[2]Mouse Phenotyping Core, Baylor College of Medicine, Houston, Texas, USA

[3]Department of Pathology and Genomic Medicine, Houston Methodist Hospital, Houston, Texas, USA

Abstract

Pulmonary hypertension (PH) frequently occurs in infants with bronchopulmonary dysplasia (BPD), causing increased mortality and right ventricular (RV) dysfunction that persists into adulthood. A first step in developing better therapeutic options is identifying and characterizing an appropriate animal model. Previously, we characterized the short-term morbidities of a model in which C57BL/6J wild-type (WT) mice were exposed to 70% O_2 (hyperoxia) during the neonatal period. Here, we aimed to determine the long-term morbidities using lung morphometry, echocardiography (Echo), and cardiac magnetic resonance imaging (cMRI). The major highlight of this study is the use of the state-of-the art imaging technique, cMRI, in mice to characterize the long-term cardiac effects of neonatal hyperoxia exposure. To this end, WT mice were exposed to 21% O_2 (normoxia) or hyperoxia for two weeks of life, followed by recovery in normoxia for six weeks. Alveolarization, pulmonary vascularization, pulmonary hypertension, and RV function were quantified at eight weeks. We found that hyperoxia exposure resulted in persistent alveolar and pulmonary vascular simplification. Furthermore, the Echo and cMRI studies demonstrated that hyperoxia-exposed mice had signs of PH and RV dysfunction as indicated by increased RV pressure, mass, and end-systolic and -diastolic volumes, and decreased RV stroke volume and ejection fractions. Taken together, our results demonstrate that neonatal hyperoxia exposure in mice cause cardiopulmonary morbidities that persists into adulthood and provides evidence for the use of this model to develop novel therapies for BPD infants with PH.

[*]Corresponding author: Neonatology Section, Baylor College of Medicine, 1102 Bates Avenue, Houston, Texas 77030, Tel: 1-832-824-6474; shivanna@bcm.edu.

Disclosures

The authors report no conflicts of interest in this work.

Keywords

Hyperoxia; Bronchopulmonary dysplasia; Pulmonary Hypertension; Echocardiography; Cardiac Magnetic Resonance Imaging; Long-term Morbidities

1 Introduction

Bronchopulmonary dysplasia (BPD) is a multi-factorial chronic lung disease of preterm infants that is characterized by interrupted lung development (Jobe, 1999). Despite improved therapies for preterm infants with respiratory failure, BPD remains the most common chronic morbidity in these patients (Fanaroff et al., 2007; Van Marter, 2009). The histopathological characteristics of BPD are alveolar and pulmonary vascular simplification (Coalson, 2003; Husain et al., 1998). Importantly, BPD-associated cardiopulmonary morbidities persist later in life (Islam et al., 2015; Simpson et al., 2015). Moreover, BPD infants who develop pulmonary hypertension (PH) have increased short- and long-term mortality and respiratory morbidities (Mourani and Abman, 2015). Finally, these patients have an increased risk of developing PH and right ventricular (RV) dysfunction later in life (Davidson and Berkelhamer, 2017; de Wijs-Meijler et al., 2017; Kwon et al., 2016), causing a significant health care- and economic-burden that lasts beyond the neonatal period. Therefore, there is a need to develop improved therapies for these patients; however, these efforts have been hindered by a lack of understanding of the molecular mechanisms contributing to the disease pathogenesis. As such, an initial step would be to comprehensively characterize the short- and long-term cardiopulmonary morbidities in small animal models of BPD with PH, and validate that this is an accurate model of human BPD with PH.

Excessive supplemental oxygen (O_2) use or hyperoxia leads to BPD and PH by disrupting growth factor signaling, extracellular matrix assembly, cell proliferation, and vasculogenesis (Madurga et al., 2013). Several studies (Aslam et al., 2009; Chen et al., 2011; Lee et al., 2013), including ours (Reynolds et al., 2016), have demonstrated that hyperoxia-induced lung parenchymal and vascular injury in neonatal mice leads to a phenotype similar to that of human BPD with PH. Moreover, preclinical studies have consistently shown that neonatal hyperoxia exposure causes decreased alveolarization and lung vascularization that persists into adulthood (Dauger et al., 2003; Mankouski et al., 2017; O'Reilly et al., 2014; Wilson et al., 1985; Yee et al., 2011). However, whether this exposure similarly causes PH and RV dysfunction in adulthood is not well studied.

The gold standard for the diagnosis of PH is cardiac catheterization. However, in neonatal mice this is a technically challenging and terminal procedure, which precludes long-term studies. Therefore, noninvasive imaging techniques such as transthoracic echocardiography (Echo) and cardiac magnetic resonance imaging (cMRI) have been increasingly used to phenotype the structure and function of the rodent heart. Echo is noninvasive, inexpensive, quick, and ideal for follow-up studies. However, it is very operator-dependent and obtaining an optimal acoustic window may be challenging in small animals. In addition, it relies on geometric assumptions, which can be altered in diseased states (Reiter et al., 2004). In

contrast, cMRI is less operator dependent, does not rely on geometric assumptions, can reliably phenotype cardiovascular structures without interference from adjacent bone or air, and more importantly has good reproducibility (Hung et al., 2009; Prasad et al., 2004). However, cMRI requires specialized animal scanners, is expensive, and more time-consuming compared with Echo. In humans, PH is diagnosed by the presence of increased pulmonary artery and RV systolic pressure (RVSP), which is estimated indirectly from tricuspid regurgitation (TR) peak flow velocity, using Echo (McLaughlin et al., 2009). Due to technical limitations preventing proper flow alignment, the measurement of TR by Doppler is inaccurate in mice. Furthermore, TR is rare in rodents and occurs only with severe PH (Jones et al., 2002). Therefore, RV systolic time intervals such as pulmonary acceleration time (PAT), ejection time (ET), and velocity time integral (VTI), which can be accurately obtained by pulsed-wave doppler (PWD) Echo are used as alternative indices of pulmonary artery pressure in rodents (Reynolds et al., 2016; Thibault et al., 2010; Urboniene et al., 2010). Echo and cMRI are noninvasive techniques that can reliably diagnose PH, quantify RV function, and circumvent the problems associated with catheterization in mice (Breen et al., 2016; Cero et al., 2015; Janssen et al., 2015; Thibault et al., 2010; Urboniene et al., 2010). Thus, the main objectives of this study were to determine the long-term cardio-pulmonary effects of neonatal hyperoxia exposure in a mouse model of experimental BPD with PH, and provide robust evidence that this animal model can be used to study the molecular mechanisms contributing to BPD and PH in infants. Based on clinical data showing that hyperoxia contributes to the development of BPD with PH and that these infants are at an increased risk for long-term cardiopulmonary morbidities, we hypothesized that exposure of neonatal C57BL/6J wild-type (WT) mice to 70% O_2 (hyperoxia) for 14 d would lead to alveolar and pulmonary vascular simplification, along with PH and RV dysfunction that persists into adulthood.

2 Materials and Methods

2.1 Animals

This study was approved and conducted in strict accordance with the federal guidelines for the humane care and use of laboratory animals by the Institutional Animal Care and Use Committee of Baylor College of Medicine. WT mice were obtained from The Jackson Laboratory (Bar Harbor, ME). Timed-pregnant mice raised in our animal facility were used for the experiments.

2.2 Hyperoxia experiments

Within 24 h of birth, WT dams and their male and female pups were exposed to 70% O_2 (hyperoxia, $n = 12$) for two weeks and then allowed to recover in 21% O_2 (normoxia) for an additional six weeks. Another group of WT dams with their pups were maintained in 21% O_2 (normoxia, $n = 12$) for eight weeks. The dams were rotated between air- and hyperoxia-exposed litters every 24 h during the hyperoxia exposure period to prevent oxygen toxicity in the dams and to control formaternal effects between the groups.

2.3 Lung morphometry and analyses of pulmonary vascularization

Alveolar development on selected mice (n = 6/exposure) was evaluated by radial alveolar counts (RAC) and mean linear intercepts (MLI) as described previously (Shivanna et al., 2013). Pulmonary vessel density was also determined in these animals based on immunohistochemical staining for von Willebrand factor (vWF), which is an endothelial specific marker (n = 6/exposure). The observers performing these measurements were masked to the slide identity.

2.4 Transthoracic Echo

The indices of PH were assessed by performing functional Echo (Reynolds et al., 2016) at eight weeks of life. Briefly, the mice (n = 6/exposure) were subjected to 2-D and pulsed-wave Doppler (PWD) Echo using the VisualSonics Vevo 2100 machine and a 40 MHz linear transducer. PWD recording of the pulmonary blood flow was obtained at the level of the aortic valve in the parasternal aortic valve right ventricular outflow view (Thibault et al., 2010) to measure PAT (defined as the time from the onset of flow to peak velocity), RV ET (the time from the onset to the termination of pulmonary flow), and pulmonary flow VTI. Based on a previous Echo study in mice, the RVSP was calculated using the regression formula RVSP = 64.5 – (83.5 x PAT/ET) (Thibault et al., 2010). These measurements were done by two independent observers who were masked to the experimental conditions.

2.5 cMRI

Cardiac function was assessed by cMRI at eight weeks of life (n = 6/exposure). The mice were anesthetized with 3% isoflurane (mixed with oxygen) and maintained with 1–2% isoflurane. Respiratory- and cardiac-gated images were acquired at end-diastole and end-systole using a 7.0T, Bruker Pharmascan, 22-mm to center-bore horizontal scanner. The imaging parameters to acquire cardiac- and respiratory-gated spin echo images were as follows: repetition time: 5.7 ms; echo time: 2.8 ms; number of slices: 6; and slice thickness: 1.0 mm. The multi-slice scan was performed in the axial orientation to visualize the left and right ventricles, and data were analyzed using Amira 3D image processing software (Mercury Computer Systems, Chelmsford, MA). The areas representing the left and right ventricular space in each slice were summated in the amount of pixels. The volume size of the space was calculated by using the known volume size of each pixel. The RV mass was determined as described previously (Redgrave et al., 2016; Urboniene et al., 2010). The observer performing the studies and measurements was masked to the experimental conditions.

2.6 Statistical Analyses

The results were analyzed using GraphPad Prism 5 software (La Jolla, CA, USA). The data are expressed as mean ± SD. The effects of exposure for the outcome variables, including alveolarization, pulmonary vascularization, PH, and cardiac function were analyzed using the two-tailed Student's t-test. A p value of < 0.05 was considered significant.

3 Results and Discussion

In this study, we investigated the long-term pulmonary and cardiovascular effects of mice who were exposed to 70% O_2 for two weeks in the neonatal period. Specifically, we assessed the effects of neonatal hyperoxia exposure on alveolarization, pulmonary vascularization, PH, and RV function in adulthood. Previously, we demonstrated that this exposure model mimics the lung phenotype of BPD infants with PH in the neonatal period (Reynolds et al., 2016). Therefore, we chose the same model for this study and found that neonatal hyperoxia exposure causes lung development abnormalities, PH, and RV dysfunction that persists into adulthood.

Hyperoxia is known to inhibit alveolar development in preterm infants (Jobe, 1999) and newborn mice (Warner et al., 1998) by disrupting signaling pathways critical for lung development (Silva et al., 2015). The mouse lungs at birth are in the saccular stage of development, which is equivalent to the developmental lung stage of a 25–26 wk preterm infant (Zoetis and Hurtt, 2003). Therefore, mice are one of the most commonly utilized laboratory animals to model human developmental lung disease such as BPD. We recently showed that neonatal hyperoxia exposure-induced alveolar and pulmonary vascular development abnormalities persists at four weeks of life (Menon et al., 2017). Because BPD infants have anatomical lung abnormalities that persist into adulthood, we evaluated the effects of neonatal hyperoxia exposure on alveolar and pulmonary vascular morphology in mice at eight weeks of age (equivalent to a human age of 21.5 years; (Dutta and Sengupta, 2016)). Adult mice exposed to neonatal hyperoxia had decreased RACs (Figure 1, A, B, and C), indicating that their alveoli were fewer in number compared with normoxia-exposed (control) animals. In addition, hyperoxia-exposed mice had significant increases in MLIs (Figure 1, A, B, and D), indicating that their alveoli were also larger than those of controls. Similarly we found that adult mice exposed to neonatal hyperoxia had decreased number of vWF-stained lung blood vessels (Figure 1, E, F, and G) compared with controls. Our findings indicate that neonatal hyperoxia exposure causes persistent alveolar and pulmonary vascular simplification, and suggests that our mouse model mimics the long-term lung phenotype of BPD infants.

Small animal models are used to discover novel therapies for many diseases because they offer a practical approach to study the pathogenic molecular mechanisms of a disease. Recently, we observed that neonatal mice exposed to 70% O_2 display echo evidence of PH at two weeks of life (Reynolds et al., 2016). However, clinical studies indicate that BPD infants continue to have cardio-respiratory morbidities in their adulthood (Davidson and Berkelhamer, 2017; de Wijs-Meijler et al., 2017; Kwon et al., 2016). Therefore, we performed two noninvasive studies, high-resolution Echo and cMRI, to investigate whether mice with hyperoxic lung injury in the neonatal period continue to have PH and RV dysfunction as adults. In agreement with the clinical studies, we find that adult mice exposed to neonatal hyperoxia display indices of both PH and RV dysfunction.

In humans and rodents, PAT has shown to inversely correlate with pulmonary artery pressures (Dabestani et al., 1987; Hansmann et al., 2012; Kitabatake et al., 1983; Urboniene et al., 2010; Vadivel et al., 2014). Further, reductions in PAT decreases PAT/ET ratio. We

observed that both PAT (Figure 2, A, B, and C) and the PAT/ET ratio (Figure 2, A, B, and D) were decreased by 20%, resulting in an asymmetric flow pattern (Figure 2, A and B), in adult mice who were exposed to neonatal hyperoxia compared with controls. Similarly, the VTI was decreased by 20% in the hyperoxia group (Figure 2E). Consistent with a prior murine model of PH (Thibault et al., 2010), the estimated RVSP was increased by 20% in hyperoxia-exposed mice (Figure 2F). There was no significant difference in the heart rate between the two groups (Figure. 2G). The interobserver variability of PAT, ET, and VTI was 5.3%, 3.3%, and 4.5%, respectively. Our Echo studies show that mice exposed to neonatal hyperoxia continued to have signs of PH in adulthood. It is important to note that the development of PH phenotype may be determined by the mouse strain and cumulative oxygen exposure. For example, exposure of neonatal C57BL6J and FVB mice to 70–75% O_2 for 14 d causes PH (Hansmann et al., 2012; Reynolds et al., 2016), whereas exposure of neonatal C3H/HeN mice to 85% O_2 for a similar duration does not cause PH (Velten et al., 2011).

cMRI has been increasingly used to assess RV function and PH in rodents subjected to several insults, including hypoxia, vascular endothelial growth factor receptor antagonist, monocrotaline, 5-hydroxytryptamine receptor antagonist, and pressure overload (Breen et al., 2016; Cero et al., 2015; Janssen et al., 2015; Novoyatleva et al., 2013; Urboniene et al., 2010). In early stages of PH, the RV maintains the stroke volume (SV) by enhancing contractility. This process, wherein the RV adapts to increased pulmonary vascular pressure to maintain the forward flow, is called ventriculoarterial coupling. In the advanced disease, uncoupling occurs and the RV attempts to maintain the SV with ventricular dilation (Kuehne et al., 2004; Vonk Noordegraaf et al., 2017). In a recent clinical study, Shang et al. (Shang et al., 2017) showed that the RV end systolic volume (ESV) and end diastolic volume (EDV) correlate positively with the severity of PH, while RV ejection fraction (EF) correlates negatively with the PH severity when RV-pulmonary uncoupling occurs. Similarly, Breen et al. (Breen et al., 2016) performed MRI studies on a adult mouse model of PH and demonstrated that the RV EDV and ESV were higher, and the RV EF was lower, in the PH group. Moreover, other preclinical studies have shown that RV EF correlates inversely with pulmonary artery pressure (Buonincontri et al., 2014; Novoyatleva et al., 2013). Our cMRI studies also showed that the RV ESV (Figure 3, A, B, and E), RV EDV (Figure 3, C, D, and F), and RV mass (Figure 3, G) were increased by 40%, 30%, and 42%, respectively, in adult mice exposed to neonatal hyperoxia, compared with controls. Additionally, the RV SV (Figure 3H) and EF (Figure 3I) were decreased by 40% and 30%, respectively, in the hyperoxia group compared with controls. To the best of our knowledge, this is the first study to characterize the long-term cardiovascular morbidities by Echo and cMRI in mice exposed to neonatal hyperoxia.

We recognize our study limitations. For one, our sample size calculation was not powered to detect gender specific differences in our study. Further, due to technical difficulties in obtaining electrocardiograph gated cMRI sequences, we were unable to quantify cardiac output and cardiac index. Lastly, we did not perform lung function tests in our experimental animals. Our future studies will address these limitations.

In summary, our study demonstrates that the long-term cardiopulmonary morbidities associated with this mouse model of experimental BPD and PH are similar to those observed in BPD infants with PH. Furthermore, we demonstrated the feasibility of using Echo and cMRI to characterize PH and RV dysfunction in mice. Therefore, this animal model may offer an opportunity to identify the pathophysiological mechanisms that contribute to BPD and PH in preterm infants. Additionally, our results suggest that this model could be used to develop therapeutic strategies to prevent and/or treat BPD with PH, and its sequelae. Finally, our findings are applicable to other PH-related research areas, such as congenital diaphragmatic hernia and congenital lung hypoplasia.

Acknowledgments

Funding

This work was supported by National Institutes of Health grants: HD-073323 to B.S., U54 HG006348 to the Mouse Phenotyping Core at Baylor College of Medicine (BCM), and P30DK056338 to the Digestive Disease Center Core at BCM, and grants from the American Heart Association BGIA-20190008 and American Lung Association RG-349917 to B.S.

We thank Pamela Parsons for her timely processing of histopathology slides.

Abbreviations

BPD	bronchopulmonary dysplasia
cMRI	cardiac magnetic resonance imaging
Echo	transthoracic echocardiography
EDV	end diastolic volume
EF	ejection fraction
ESV	end systolic volume
ET	ejection time
MLI	mean linear intercepts
O_2	oxygen
PAT	pulmonary acceleration time
PH	pulmonary hypertension
PWD	pulsed-wave Doppler
RAC	radial alveolar count
RV	right ventricle
SV	stroke volume
TR	tricuspid regurgitation

WT	wild type
VTI	velocity time integral
vWF	von Willebrand factor

References

Aslam M, Baveja R, Liang OD, Fernandez-Gonzalez A, Lee C, Mitsialis SA, Kourembanas S. Bone marrow stromal cells attenuate lung injury in a murine model of neonatal chronic lung disease. American journal of respiratory and critical care medicine. 2009; 180(11):1122–1130. [PubMed: 19713447]

Breen EC, Scadeng M, Lai NC, Murray F, Bigby TD. Functional magnetic resonance imaging for In Vivo quantification of pulmonary hypertension in the Sugen 5416/hypoxia mouse. Experimental physiology. 2016

Buonincontri G, Wood NI, Puttick SG, Ward AO, Carpenter TA, Sawiak SJ, Morton AJ. Right ventricular dysfunction in the R6/2 transgenic mouse model of Huntington's disease is unmasked by dobutamine. Journal of Huntington's disease. 2014; 3(1):25–32.

Cero FT, Hillestad V, Sjaastad I, Yndestad A, Aukrust P, Ranheim T, Lunde IG, Olsen MB, Lien E, Zhang L, Haugstad SB, Loberg EM, Christensen G, Larsen KO, Skjonsberg OH. Absence of the inflammasome adaptor ASC reduces hypoxia-induced pulmonary hypertension in mice. American journal of physiology Lung cellular and molecular physiology. 2015; 309(4):L378–387. [PubMed: 26071556]

Chen S, Rong M, Platteau A, Hehre D, Smith H, Ruiz P, Whitsett J, Bancalari E, Wu S. CTGF disrupts alveolarization and induces pulmonary hypertension in neonatal mice: implication in the pathogenesis of severe bronchopulmonary dysplasia. American journal of physiology Lung cellular and molecular physiology. 2011; 300(3):L330–340. [PubMed: 21239535]

Coalson JJ. Pathology of new bronchopulmonary dysplasia. Seminars in neonatology: SN. 2003; 8(1): 73–81. [PubMed: 12667832]

Dabestani A, Mahan G, Gardin JM, Takenaka K, Burn C, Allfie A, Henry WL. Evaluation of pulmonary artery pressure and resistance by pulsed Doppler echocardiography. The American journal of cardiology. 1987; 59(6):662–668. [PubMed: 3825910]

Dauger S, Ferkdadji L, Saumon G, Vardon G, Peuchmaur M, Gaultier C, Gallego J. Neonatal exposure to 65% oxygen durably impairs lung architecture and breathing pattern in adult mice. Chest. 2003; 123(2):530–538. [PubMed: 12576377]

Davidson LM, Berkelhamer SK. Bronchopulmonary Dysplasia: Chronic Lung Disease of Infancy and Long-Term Pulmonary Outcomes. Journal of clinical medicine. 2017; 6(1)

de Wijs-Meijler DP, Duncker DJ, Tibboel D, Schermuly RT, Weissmann N, Merkus D, Reiss IKM. Oxidative injury of the pulmonary circulation in the perinatal period: Short- and long-term consequences for the human cardiopulmonary system. Pulmonary circulation. 2017; 7(1):55–66. [PubMed: 28680565]

Dutta S, Sengupta P. Men and mice: Relating their ages. Life sciences. 2016; 152:244–248. [PubMed: 26596563]

Fanaroff AA, Stoll BJ, Wright LL, Carlo WA, Ehrenkranz RA, Stark AR, Bauer CR, Donovan EF, Korones SB, Laptook AR, Lemons JA, Oh W, Papile LA, Shankaran S, Stevenson DK, Tyson JE, Poole WK. Trends in neonatal morbidity and mortality for very low birthweight infants. Am J Obstet Gynecol. 2007; 196(2):147, e141–148. [PubMed: 17306659]

Hansmann G, Fernandez-Gonzalez A, Aslam M, Vitali SH, Martin T, Mitsialis SA, Kourembanas S. Mesenchymal stem cell-mediated reversal of bronchopulmonary dysplasia and associated pulmonary hypertension. Pulmonary circulation. 2012; 2(2):170–181. [PubMed: 22837858]

Hung J, Francois C, Nelson NA, Young A, Cowan BR, Jerecic R, Carr J. Cardiac image modeling tool for quantitative analysis of global and regional cardiac wall motion. Investigative radiology. 2009; 44(5):271–278. [PubMed: 19346964]

Husain AN, Siddiqui NH, Stocker JT. Pathology of arrested acinar development in postsurfactant bronchopulmonary dysplasia. Human pathology. 1998; 29(7):710–717. [PubMed: 9670828]

Islam JY, Keller RL, Aschner JL, Hartert TV, Moore PE. Understanding the Short- and Long-Term Respiratory Outcomes of Prematurity and Bronchopulmonary Dysplasia. American journal of respiratory and critical care medicine. 2015; 192(2):134–156. [PubMed: 26038806]

Janssen W, Schymura Y, Novoyatleva T, Kojonazarov B, Boehm M, Wietelmann A, Luitel H, Murmann K, Krompiec DR, Tretyn A, Pullamsetti SS, Weissmann N, Seeger W, Ghofrani HA, Schermuly RT. 5-HT2B receptor antagonists inhibit fibrosis and protect from RV heart failure. BioMed research international. 2015; 2015:438403. [PubMed: 25667920]

Jobe AJ. The new BPD: an arrest of lung development. Pediatric research. 1999; 46(6):641–643. [PubMed: 10590017]

Jones JE, Mendes L, Rudd MA, Russo G, Loscalzo J, Zhang YY. Serial noninvasive assessment of progressive pulmonary hypertension in a rat model. American journal of physiology Heart and circulatory physiology. 2002; 283(1):H364–371. [PubMed: 12063310]

Kitabatake A, Inoue M, Asao M, Masuyama T, Tanouchi J, Morita T, Mishima M, Uematsu M, Shimazu T, Hori M, Abe H. Noninvasive evaluation of pulmonary hypertension by a pulsed Doppler technique. Circulation. 1983; 68(2):302–309. [PubMed: 6861308]

Kuehne T, Yilmaz S, Steendijk P, Moore P, Groenink M, Saaed M, Weber O, Higgins CB, Ewert P, Fleck E, Nagel E, Schulze-Neick I, Lange P. Magnetic resonance imaging analysis of right ventricular pressure-volume loops: in vivo validation and clinical application in patients with pulmonary hypertension. Circulation. 2004; 110(14):2010–2016. [PubMed: 15451801]

Kwon HW, Kim HS, An HS, Kwon BS, Kim GB, Shin SH, Kim EK, Bae EJ, Noh CI, Choi JH. Long-Term Outcomes of Pulmonary Hypertension in Preterm Infants with Bronchopulmonary Dysplasia. Neonatology. 2016; 110(3):181–189. [PubMed: 27172918]

Lee KJ, Berkelhamer SK, Kim GA, Taylor JM, O'Shea KM, Steinhorn RH, Farrow KN. Disrupted Pulmonary Artery cGMP Signaling in Mice with Hyperoxia-Induced Pulmonary Hypertension. Am J Respir Cell Mol Biol. 2013

Madurga A, Mizikova I, Ruiz-Camp J, Morty RE. Recent advances in late lung development and the pathogenesis of bronchopulmonary dysplasia. American journal of physiology Lung cellular and molecular physiology. 2013; 305(12):L893–905. [PubMed: 24213917]

Mankouski A, Kantores C, Wong MJ, Ivanovska J, Jain A, Benner EJ, Mason SN, Tanswell AK, Auten RL, Jankov RP. Intermittent hypoxia during recovery from neonatal hyperoxic lung injury causes long-term impairment of alveolar development: A new rat model of BPD. American journal of physiology Lung cellular and molecular physiology. 2017; 312(2):L208–L216. [PubMed: 27913427]

McLaughlin VV, Archer SL, Badesch DB, Barst RJ, Farber HW, Lindner JR, Mathier MA, McGoon MD, Park MH, Rosenson RS, Rubin LJ, Tapson VF, Varga J, Harrington RA, Anderson JL, Bates ER, Bridges CR, Eisenberg MJ, Ferrari VA, Grines CL, Hlatky MA, Jacobs AK, Kaul S, Lichtenberg RC, Lindner JR, Moliterno DJ, Mukherjee D, Pohost GM, Rosenson RS, Schofield RS, Shubrooks SJ, Stein JH, Tracy CM, Weitz HH, Wesley DJ. ACCF/AHA 2009 expert consensus document on pulmonary hypertension: a report of the American College of Cardiology Foundation Task Force on Expert Consensus Documents and the American Heart Association: developed in collaboration with the American College of Chest Physicians, American Thoracic Society, Inc., and the Pulmonary Hypertension Association. Circulation. 2009; 119(16):2250–2294. [PubMed: 19332472]

Menon RT, Shrestha AK, Shivanna B. Hyperoxia exposure disrupts adrenomedullin signaling in newborn mice: Implications for lung development in premature infants. Biochemical and biophysical research communications. 2017; 487(3):666–671. [PubMed: 28438602]

Mourani PM, Abman SH. Pulmonary Hypertension and Vascular Abnormalities in Bronchopulmonary Dysplasia. Clinics in perinatology. 2015; 42(4):839–855. [PubMed: 26593082]

Novoyatleva T, Janssen W, Wietelmann A, Schermuly RT, Engel FB. TWEAK/Fn14 axis is a positive regulator of cardiac hypertrophy. Cytokine. 2013; 64(1):43–45. [PubMed: 23764551]

O'Reilly M, Harding R, Sozo F. Altered small airways in aged mice following neonatal exposure to hyperoxic gas. Neonatology. 2014; 105(1):39–45. [PubMed: 24281398]

Prasad SK, Kotwinski P, Assomul R. The role of cardiovascular magnetic resonance in the evaluation of patients with heart failure. Expert review of cardiovascular therapy. 2004; 2(1):53–59. [PubMed: 15038413]

Redgrave RE, Tual-Chalot S, Davison BJ, Greally E, Santibanez-Koref M, Schneider JE, Blamire AM, Arthur HM. Using MRI to predict future adverse cardiac remodelling in a male mouse model of myocardial infarction. International journal of cardiology Heart & vasculature. 2016; 11:29–34. [PubMed: 27882341]

Reiter G, Reiter U, Rienmuller R, Gagarina N, Ryabikin A. On the value of geometry-based models for left ventricular volumetry in magnetic resonance imaging and electron beam tomography: a Bland-Altman analysis. European journal of radiology. 2004; 52(2):110–118. [PubMed: 15489068]

Reynolds CL, Zhang S, Shrestha AK, Barrios R, Shivanna B. Phenotypic assessment of pulmonary hypertension using high-resolution echocardiography is feasible in neonatal mice with experimental bronchopulmonary dysplasia and pulmonary hypertension: a step toward preventing chronic obstructive pulmonary disease. International journal of chronic obstructive pulmonary disease. 2016; 11:1597–1605. [PubMed: 27478373]

Shang X, Xiao S, Dong N, Lu R, Wang L, Wang B, Chen Y, Zhong L, Liu M. Assessing right ventricular function in pulmonary hypertension patients and the correlation with the New York Heart Association (NYHA) classification. Oncotarget. 2017

Shivanna B, Zhang W, Jiang W, Welty SE, Couroucli XI, Wang L, Moorthy B. Functional deficiency of aryl hydrocarbon receptor augments oxygen toxicity-induced alveolar simplification in newborn mice. Toxicology and applied pharmacology. 2013; 267(3):209–217. [PubMed: 23337360]

Silva DM, Nardiello C, Pozarska A, Morty RE. Recent advances in the mechanisms of lung alveolarization and the pathogenesis of bronchopulmonary dysplasia. American journal of physiology Lung cellular and molecular physiology. 2015; 309(11):L1239–1272. [PubMed: 26361876]

Simpson SJ, Hall GL, Wilson AC. Lung function following very preterm birth in the era of ‘new’ bronchopulmonary dysplasia. Respirology (Carlton, Vic). 2015; 20(4):535–540.

Thibault HB, Kurtz B, Raher MJ, Shaik RS, Waxman A, Derumeaux G, Halpern EF, Bloch KD, Scherrer-Crosbie M. Noninvasive assessment of murine pulmonary arterial pressure: validation and application to models of pulmonary hypertension. Circulation Cardiovascular imaging. 2010; 3(2):157–163. [PubMed: 20044514]

Urboniene D, Haber I, Fang YH, Thenappan T, Archer SL. Validation of high-resolution echocardiography and magnetic resonance imaging vs. high-fidelity catheterization in experimental pulmonary hypertension. American journal of physiology Lung cellular and molecular physiology. 2010; 299(3):L401–412. [PubMed: 20581101]

Vadivel A, Alphonse RS, Ionescu L, Machado DS, O’Reilly M, Eaton F, Haromy A, Michelakis ED, Thebaud B. Exogenous hydrogen sulfide (H2S) protects alveolar growth in experimental O2-induced neonatal lung injury. PloS one. 2014; 9(3):e90965. [PubMed: 24603989]

Van Marter LJ. Epidemiology of bronchopulmonary dysplasia. Seminars in fetal & neonatal medicine. 2009; 14(6):358–366. [PubMed: 19783238]

Velten M, Hutchinson KR, Gorr MW, Wold LE, Lucchesi PA, Rogers LK. Systemic maternal inflammation and neonatal hyperoxia induces remodeling and left ventricular dysfunction in mice. PloS one. 2011; 6(9):e24544. [PubMed: 21935422]

Vonk Noordegraaf A, Westerhof BE, Westerhof N. The Relationship Between the Right Ventricle and its Load in Pulmonary Hypertension. Journal of the American College of Cardiology. 2017; 69(2): 236–243. [PubMed: 28081831]

Warner BB, Stuart LA, Papes RA, Wispe JR. Functional and pathological effects of prolonged hyperoxia in neonatal mice. Am J Physiol. 1998; 275(1 Pt 1):L110–117. [PubMed: 9688942]

Wilson WL, Mullen M, Olley PM, Rabinovitch M. Hyperoxia-induced pulmonary vascular and lung abnormalities in young rats and potential for recovery. Pediatric research. 1985; 19(10):1059–1067. [PubMed: 2932674]

Yee M, White RJ, Awad HA, Bates WA, McGrath-Morrow SA, O'Reilly MA. Neonatal hyperoxia causes pulmonary vascular disease and shortens life span in aging mice. The American journal of pathology. 2011; 178(6):2601–2610. [PubMed: 21550015]

Zoetis T, Hurtt ME. Species comparison of lung development. Birth defects research Part B, Developmental and reproductive toxicology. 2003; 68(2):121–124. [PubMed: 12866703]

Highlights

- Magnetic resonance imaging can reliably phenotype murine right ventricular function.
- Neonatal hyperoxia exposure leads to persistent pulmonary hypertension in mice.
- Adult mice exposed to neonatal hyperoxia also display right ventricular dysfunction.
- Neonatal hyperoxia exposure causes persistent lung developmental defects in mice.

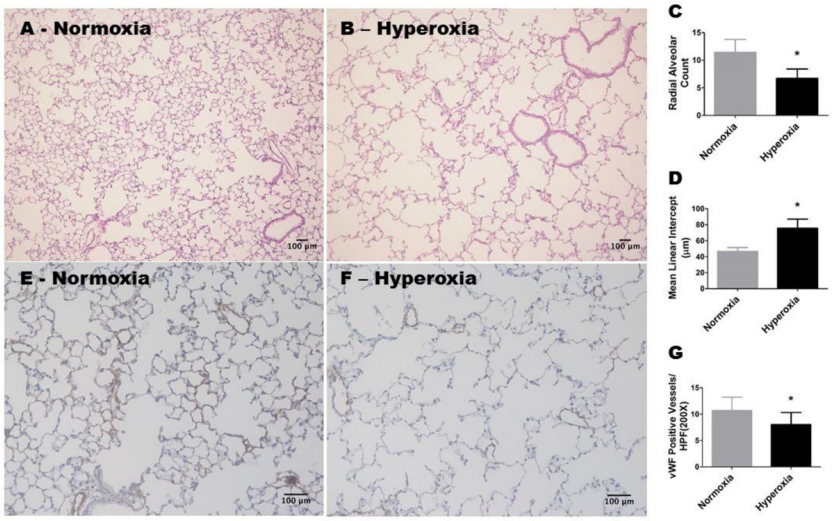

Figure 1. Alveolar and pulmonary vascular development continues to be interrupted in adult mice exposed to hyperoxia during the neonatal period

WT mice were exposed to either 21 % O2 (normoxia) for 8 weeks, or 70 % O2 (hyperoxia) for 2 weeks followed by normoxia for 6 weeks (n = 6 mice/group). A and B: Representative hematoxylin and eosin-stained lung sections (100x magnification). C: Radial alveolar counts. D: Mean linear intercepts. E and F: Representative von Willebrand Factor (vWF)-stained lung blood vessels (200x magnification). G: Quantitative analysis of vWF-stained lung blood vessels per high power field (HPF). Values are presented as the mean ± SD. Significant differences between normoxia- and hyperoxia-exposed mice are indicated by *, $p < 0.05$ (t-test). Scale bar = 100 μM.

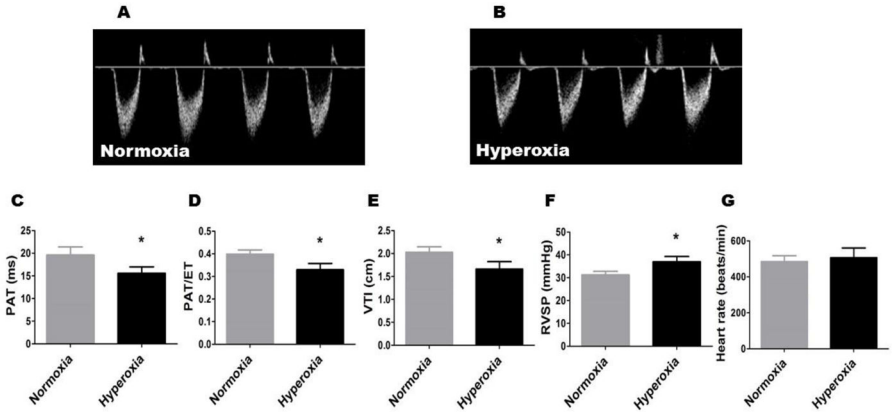

Figure 2. Echo findings of persistent PH in adult mice exposed to neonatal hyperoxia

A and B: Representative PWD Echo recordings of pulmonary artery blood flow obtained in 8-week-old mice who were exposed to normoxia (A) or hyperoxia (B) in the neonatal period. C–E: PAT (C), PAT/ET ratio (D), VTI (E), RVSP (F), and heart rate (G) were estimated from the PWD Echo recordings of the pulmonary artery blood flow. Values are presented as mean ± SD (n = 6 mice/group). Significant differences between normoxia and hyperoxia groups are indicated by *, $p < 0.05$ (t-test).

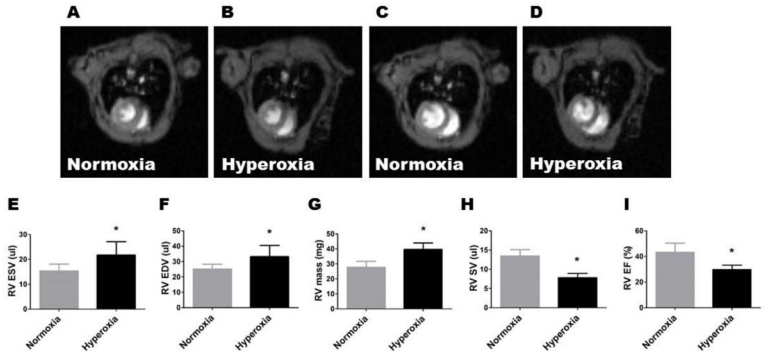

Figure 3. Adult mice exposed to neonatal hyperoxia have RV dysfunction

Eight-week-old mice who were exposed to normoxia or hyperoxia in the neonatal period were analyzed by cMRI. A–D: Representative images of the heart at end systole (A–B) and end diastole (C–D). E–I: The quantitative analyses of end systolic volume (ESV; E), end diastolic volume (EDV; F), RV mass (G), RV stroke volume (RVSV; H), and RV ejection fraction (RVEF; I). Values are presented as mean ± SD (n = 6 mice/group). Significant differences between normoxia and hyperoxia groups are indicated by *, $p < 0.05$ (t-test).